

Flaring loop structures at VLBI scale in UX Arietis

E. Franciosini¹, M. Massi^{2,3}, J.M. Paredes⁴, and R. Estalella⁴

¹ Dipartimento di Astronomia e Scienza dello Spazio, Università di Firenze, Largo E. Fermi 5, I-50125 Florence, Italy

² Max-Planck-Institut für Radioastronomie, Auf dem Hügel 69, D-53121 Bonn, Germany

³ Joint Institute for VLBI in Europe, Postbus 2, 7990 AA Dwingeloo, The Netherlands

⁴ Departament d'Astronomia i Meteorologia, Universitat de Barcelona, Av. Diagonal 647, E-08028 Barcelona, Spain

Received 21 July 1998 / Accepted 21 October 1998

Abstract. We report the results of three VLBI observations at 5 GHz of the active binary system UX Ari. Observations have been made during five consecutive days with the aim of studying the variations of the source structure during the decay phase of a flare.

We find that during the observations UX Ari was undergoing a low-energy flare (peak flux ~ 60 mJy) with a decay time of a few days. The maps show a clear variation of the source structure with time. The visibility function and the maps can be reproduced using two gaussian components of angular dimensions $\sim 2 \times 1$ mas, whose relative position changes. Since the observations have been made at different orbital phases, we interpret the observed variations of the source structure as due to two distinct flaring loops that are seen in different positions as the star rotates.

Key words: stars: binaries: close – stars: flare – stars: individual: UX Ari – radio continuum: stars

1. Introduction

RS CVn stars are binary systems characterized by an intense coronal activity consisting in the occurrence of strong flares detected in X-rays, UV lines and at radio wavelengths. One of the most active sources at radio wavelengths is the system UX Ari, formed by a G5V and a K0IV star, with an inclination $i = 60^\circ$ and an orbital period of 6.44 days; the rotational period is very similar to the orbital one, due to tidal synchronization. The K star is the most active one and shows large spots located both near the stellar equator and the pole (e.g. Vogt & Hatzes 1991; Elias et al. 1995).

The radio emission of this system is highly variable. A monitoring program performed since December 1992 at the Effelsberg 100-m radiotelescope (Neidhöfer et al. 1993; Massi et al. 1998) has shown the presence of periods of intense activity, with strong flares occurring every few days, followed by lower activity periods when only moderate flares ($S_\nu \leq 100$ mJy) or the “quiescent” emission are observed.

Previous VLBI observations of UX Ari have shown that also the source structure is variable: during strong flares a compact

bright source of stellar size and a fainter extended component of dimensions comparable to the binary separation are observed (Mutel et al. 1985); at lower flux levels however only the extended component is present (Massi et al. 1988).

Franciosini & Chiuderi Drago (1995) developed a model in which a population of non-thermal electrons, with the power-law distribution necessary to reproduce the flare spectrum, is injected at the time $t = 0$ in a pre-existing magnetic loop and then evolves in time due to collision and synchrotron losses. The calculations of the emission at different times after the particle injection show that both the spectral index between 1 and 5 GHz and the flux density decrease with time, in very good agreement with the observations (Mutel et al. 1987). An important consequence of the above model is the evolution of the source morphology from a brighter compact region plus an extended source in the first 20 to 24 hours after the flare, to a quasi-homogeneous extended component in the following days. The initial structure is due to the fact that the emission in regions close to the stellar surface, where the magnetic field is higher (> 100 G), is more intense than far from it where the magnetic field is of the order of 5–10 G or less. On the other hand, the lifetime of relativistic particles near the stellar surface, where high plasma density and strong magnetic fields are present, is much shorter than far from it. Therefore, the compact source will disappear rapidly, while, due to the lower efficiency of radiative and collisional losses, the extended region will survive for a period of several days, emitting a flux density (the quiescent emission) that will slowly decrease until the onset of the next flare. Mutel et al. (1985) came to the same conclusion with a qualitative model considering only radiation losses of particles in an expanding loop.

VLBI observations of the evolution of the source structure during the decay phase of a flare can give a crucial confirmation of the validity of the above model. For this reason, we have performed three VLBI observations of UX Ari during a period of five consecutive days.

2. Observations

The observations were made at 5 GHz on 1993 September 11, 14 and 15 (hereafter referred as case A, B and C, respectively), using the global VLBI network. The telescopes used were: Effels-

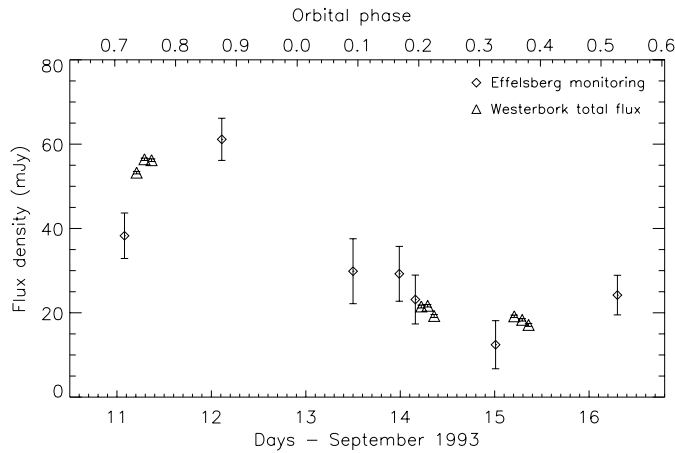


Fig. 1. Radio light curve of UX Ari at 5 GHz from September 11 to September 16. The figure shows the total flux density measured at Westerbork during the three VLBI runs, averaged over two hours (triangles), and the observations made during the Effelsberg monitoring program (diamonds; Massi et al. 1998)

berg (Germany), Jodrell Bank (UK), Westerbork (the Netherlands), Medicina and Noto (Italy), VLA (New Mexico), and three VLBA antennas located at Hancock (New Hampshire), Owens Valley (OVRO, California), and St. Croix (Virgin Islands). The fringe spacing ranged from 15 mas on the Effelsberg-Medicina baseline to 1.3 mas on the Noto-OVRO baseline.

Each observation lasted 7 hours, from 4:00 to 11:00 UT, and consisted of a series of 13 minute scans, including four 3 minute observations of the calibrator source NRAO 140. The data were recorded with Mark IIIA terminals in standard B mode, with a bandwidth of 28 MHz in left circular polarization, and were correlated at the Max Planck Institute für Radioastronomie in Bonn. The calibration was performed using the standard VLBI tasks in AIPS.

The total flux density during the three VLBI runs has been monitored at Westerbork: the data show that the flux density remained nearly constant during each observations, but its mean value decreased from 55 mJy on September 11 to 21 mJy on September 14 and to 18 mJy on September 15. During the same period, UX Ari was observed at Effelsberg at the same frequency, as part of a monitoring program (Massi et al. 1998). Fig. 1 shows the observed flux density as a function of time from September 11 to September 16; the Westerbork data have been averaged over 2 hours intervals. As it can be seen, the flux density was rising during the first VLBI run, reached a maximum ($S_\nu \sim 60 - 70$ mJy) between September 11 and 12, and then decayed to a minimum on September 15. This behaviour can be attributed to a low-energy flare which probably started just before the first VLBI run: the five days interval of the observations allowed us to follow its entire evolution until the end of its decay phase. However, since the observations cover almost a complete orbital period, it is possible that the observed flux variations are not entirely due to the flare evolution, but a contribution due to rotational modulation is present. We shall discuss this in more detail in the following sections.

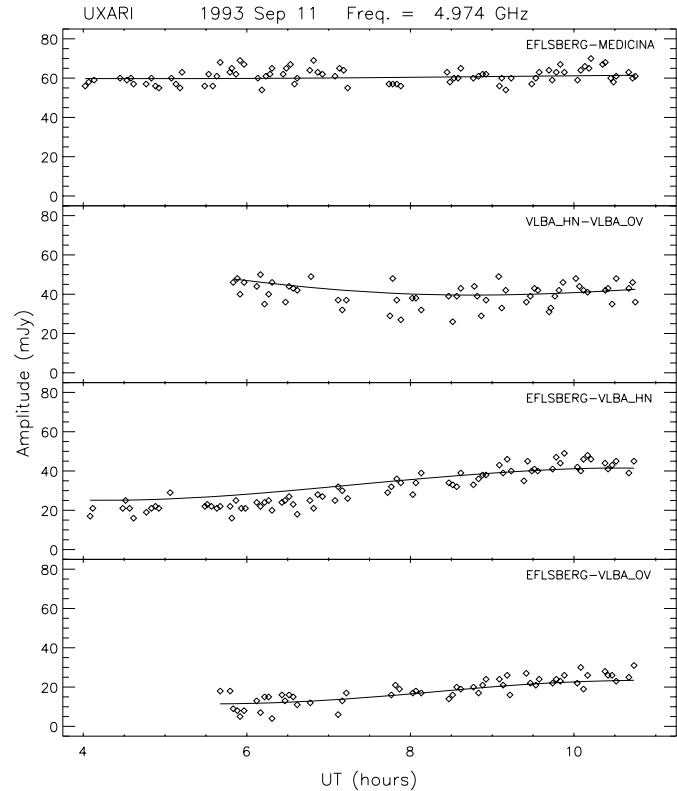


Fig. 2. Observed visibilities (diamonds) in case A (September 11) for different baselines at increasing angular resolutions θ : from top to bottom, $\theta = 16$ mas (Effelsberg-Medicina), 3.2 mas (Hancock-OVRO), 2.2 mas (Effelsberg-Hancock) and 1.5 mas (Effelsberg-OVRO). The data are averaged over 3 minute intervals. The solid line represents the model visibility function obtained using the two gaussian components of Table 1

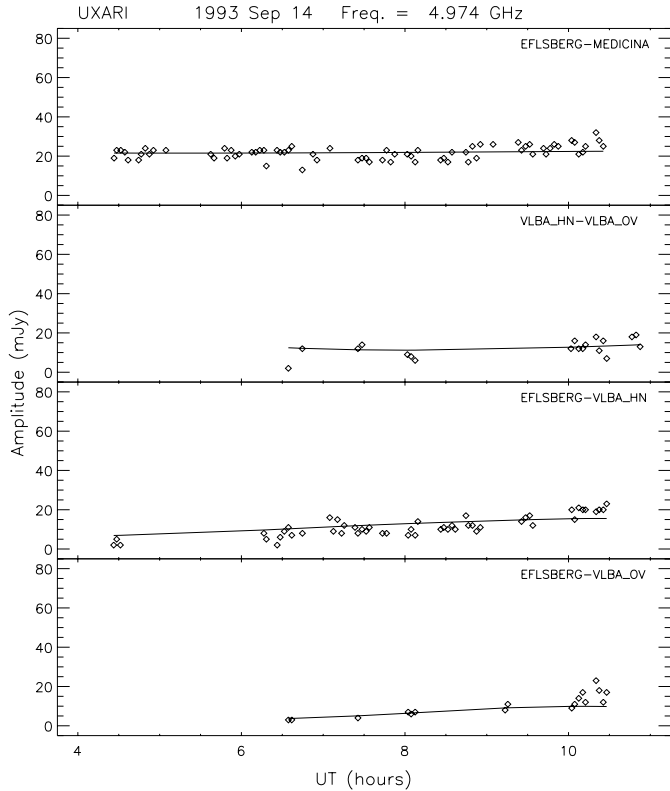
3. Results

UX Ari was detected on all baselines. The observed visibilities as a function of time during the three runs are shown in Figs. 2, 3 and 4 for some selected baselines with increasing angular resolution. The data are averaged over 3-minute intervals. In case C only two baselines are shown, since after editing and calibration only a few data points are left in the other baselines. In all cases the visibility amplitude decreases with increasing baseline length, clearly indicating that UX Ari was resolved on the longest baselines.

Fig. 5 shows the maps obtained for the three observations. In all maps the r.m.s. is $\sigma \sim 0.25$ mJy/beam and the first level corresponds to 4σ . The beam size (FWHM) is 1.8×0.7 mas in cases A and B and 2.7×1.2 mas in case C. A clear variation of the source structure with time is present. It appears that the source consists of a main component which maintains nearly the same shape as the flux density decays, and a secondary component which changes its position relative to the first one. In map C the position of the emission peak is displaced with respect to the other two maps; however, we cannot tell whether this displacement is real, since in the self-calibration process we

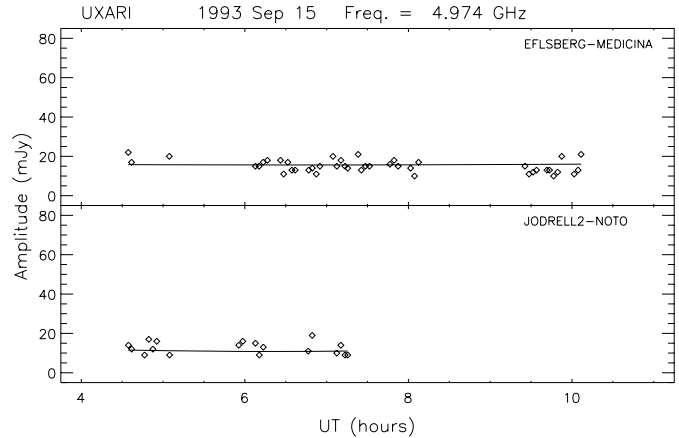
Table 1. Parameters of the two gaussian components model that best fit the observed data. The values shown refer to the unconvolved gaussian components. The last two columns show the angular separation and position angle of the second component with respect to the first one

| Date | 1st component | | | | Total flux (mJy) | 2nd component | | | Relative position | |
|---------|---------------------|--------------------|--------------------|---------------|---------------------|--------------------|--------------------|---------------|-------------------|---------------|
| | Total flux (mJy) | Maj. axis (mas) | Min. axis (mas) | P.A. (deg) | | Maj. axis (mas) | Min. axis (mas) | P.A. (deg) | Separ. (mas) | P.A. (deg) |
| 11/9/93 | 43.5 ± 1.0 | 1.8 ± 0.2 | 0.7 ± 0.1 | -20 ± 2 | 18.4 ± 1.1 | 1.7 ± 0.3 | 0.7 ± 0.5 | -80 ± 7 | 0.2 ± 0.1 | -84 ± 7 |
| 14/9/93 | 15.3 ± 0.3 | 2.0 ± 0.2 | 0.6 ± 0.1 | -25 ± 7 | 7.5 ± 0.4 | 2.2 ± 0.8 | 0.7 ± 0.6 | -80 ± 5 | 0.8 ± 0.2 | 125 ± 35 |
| 15/9/93 | 11.7 ± 0.5 | 1.5 ± 0.4 | 0.7 ± 1.0 | -45 ± 15 | 4.6 ± 0.5 | 1.8 ± 0.6 | 1.3 ± 0.9 | -70 ± 10 | 2.4 ± 0.9 | 60 ± 12 |

**Fig. 3.** Same as Fig. 2 for case B (September 14)

have lost any information on the absolute position of the radio source.

We have used the Difmap program to perform a best-fit of the visibility amplitude and phases using two elliptical gaussian components. The best agreement with the data was found using, for the unconvolved components, the parameters reported in Table 1. As it can be seen, the two components have comparable sizes of about 2×0.7 mas, corresponding to a linear size of $(1.5 \times 0.5) 10^{12}$ cm at a distance of 50 pc. This size is comparable with the binary system separation ($a = 18 R_{\odot} \simeq 1.3 10^{12}$ cm), in agreement with previous VLBI observations of RS CVn systems (Lestrade et al. 1984; Mutel et al. 1985; Massi et al. 1988; Trigilio et al. 1993; Beasley & Bastian 1996). It is interesting to note that the two components have a nearly fixed orientation on the plane of the sky, although their relative position varies, increasing their angular separation. The flux density is higher for the first component and decreases with time. The

**Fig. 4.** Same as Fig. 2 for case C (September 15). In this case only the two baselines Effelsberg-Medicina ($\theta = 16$ mas) and Jodrell-Noto ($\theta = 5$ mas) have been plotted, being the ones with more available data points

corresponding brightness temperature decreases from $2 10^9$ K to $8 10^8$ K and from $1 10^9$ K to $1 10^8$ K for the first and second component, respectively. These values are consistent with gyrosynchrotron emission from mildly relativistic electrons.

The model results for the amplitudes are shown as solid lines in Figs. 2, 3 and 4; the fit is very good at all baselines and, although not shown here, this is true also for the visibility phases. Moreover, the simulated maps obtained using the model parameters of Table 1 and shown in Fig. 6 also reproduce remarkably well the observed VLBI structure of UX Ari.

We must note that in case A the first component is very similar to the beam both in size and orientation. This situation could also be an artifact due to an unresolved component. However, from the visibility amplitude at the longest baselines we derive that, if an unresolved component is really present, its flux should not exceed 10–15 mJy; moreover, using a combination of a compact and an extended source, it is not possible to fit the visibility amplitude and simultaneously reproduce the observed map. We have performed a further check by making a new map using both a smaller elliptical beam with same position angle and a circular beam. In both cases the two extended components are clearly evident in the map, and the parameters that best fit both the visibility and the map structure are very similar to those of Table 1. We can therefore conclude that the size shown in Table 1 is the real size of the component.

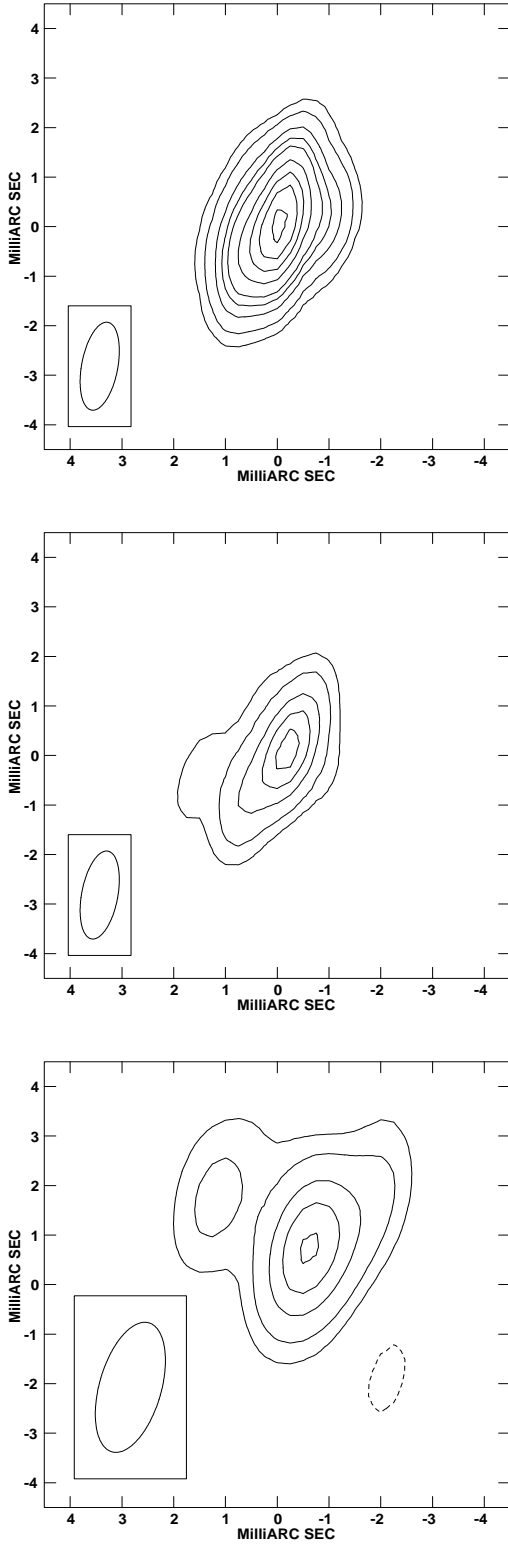


Fig. 5. VLBI maps of UX Ari obtained, from *top to bottom*, on September 11 (A), 14 (B) and 15 (C) respectively. The restoring beam size is 1.8×0.7 mas in case A and B, and 2.7×1.2 mas in case C. The r.m.s. (σ) on all maps is ~ 0.25 mJy/beam and the contours correspond to 1, 2, 4, 6, 8, 12, 16, 20, 25 mJy/beam. The peak intensity for the three maps is 27.16 (A), 9.11 (B) and 8.23 (C) mJy/beam

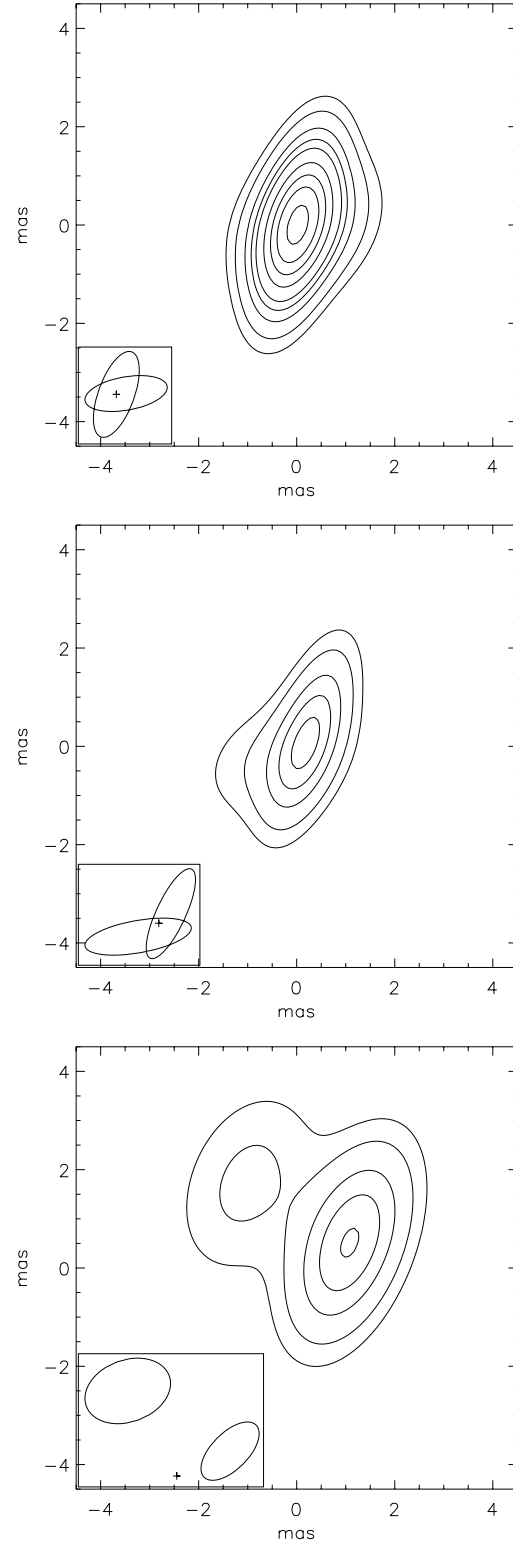


Fig. 6. Simulated maps of UX Ari for each of the three observations, obtained from the two-gaussian component model shown in Table 1 using the same restoring beam as the observations. The model peak intensity is 27.16 (A), 9.07 (B) and 8.23 (C) mJy/beam. The panel in the lower left corner shows the unconvolved gaussian components; the cross indicates the position of the map centre

4. Discussion

From Fig. 1 it is evident that at the time of our VLBI observations UX Ari was undergoing a moderate flare. In particular, the first VLBI run caught the final part of the flare rising phase, while the other two observations were made near the end of the flare decay. According to previous VLBI observations of RS CVn stars, we would expect to see a compact bright component plus an extended one at the flare peak, which evolves to an extended weaker source at the end of the flare. As mentioned in the introduction, this variation of the source structure has been interpreted by Franciosini & Chiuderi Drago (1995) by taking into account the time evolution of a population of relativistic electrons due to collision and synchrotron losses in a magnetic loop.

However there is no indication of a compact source in the first VLBI run; one of the components is indeed brighter than the other, but both are extended with approximately equal sizes. In previous VLBI observations, compact sources have generally been observed at higher flux levels. It is therefore possible that the presence of a compact source is linked with the activity of the star. A continuous monitoring of UX Ari at the Effelsberg radiotelescope (Neidhöfer et al. 1993; Massi et al. 1998) has shown that this system has an activity cycle of about 160 days, being in an active state, with strong and frequent flares, for 95 days, while for the remaining period the flux density never exceeds 100 mJy. From their data we deduce that at the time of our VLBI observations the star was in the low-activity state. However, recently Beasley & Bastian (1996) observed UX Ari with the VLBA during a strong flare, in the high-activity period, and they found only an extended component with no evidence of any compact source. Similar results were obtained for HR 1099 by Trigilio et al. (1993), although the resolution of their observation did not allow them to exclude a contribution from a compact component.

The absence of a compact component during flares can be explained by the presence of energy losses that rapidly reduce the emission from the regions of higher magnetic field near the stellar surface, that are responsible for the bright compact emission. This is true even during the rising phase. Torricelli et al. (1998) have developed a model to interpret some spectra observed during the rising phase of flares, finding that near the peak of the flare emission, when the acceleration of particles is nearly over, energy losses play an important role and there is no more emission from the lower parts of the emitting loop.

The most interesting result of our VLBI observations is the variation of the source structure: apart from the decrease of the flux density, the two components change their relative position with time. The time interval between the first and last VLBI run is 4 days, which correspond to an orbital phase variation $\Delta\phi = 0.62$ ($P_{\text{orb}} = 6.438^{\text{d}}$). We can therefore interpret the changes in the source structure as the effect of the stellar rotation. From the ephemerides by Carlos & Popper (1971), $HJD = 2440133.766 + 6.43791 E$, we have computed the mean orbital phases of the three VLBI observations, finding the values $\phi = 0.75$ (A), $\phi = 0.21$ (B) and $\phi = 0.37$ (C),

where $\phi = 0$ corresponds to conjunction with the active K star in front. Case C, which corresponds to a minimum in the light curve (see Fig. 1), is particularly interesting. Recent long-term observations of UX Ari by Massi et al. (1998) and Trigilio et al. (1998) in fact have shown evidence of a minimum in the radio emission around orbital phase 0.4–0.5, which appears to be stable over many orbital periods. Such a minimum has been interpreted assuming that the emitting source is located on the hemisphere of the K star opposite to the G star, and that it is occulted by the star during its rotation.

What can we deduce from our data about the source structure? If the observations had shown a compact and an extended component, it would have been possible to interpret the data as the emission from a single loop, with the two components associated with the loop feet and top, respectively. Our result, tested with a parallel fit on both the uv and sky planes for three independent data sets, consists instead of two extended components. It is evident that the above defined single-loop geometry becomes in our case a too simplistic model, unless one would assume an unphysical highly inhomogeneous loop.

The simplest interpretation is that the two components represent the emission from the top of two different loops located on the active star. From our data it is not possible to deduce if the peak flux observed on September 11–12 is due to the flaring of both loops, with different intensities, or if the flare occurred only in the first loop, while the emission from the other one is the residual of a previous flaring event. The observed decrease of the flux density with time can be interpreted as the decay of the flaring emission due to energy losses, according to the model by Franciosini & Chiuderi Drago (1995). According to this model, the emission from the feet has disappeared due to energy losses, and the sources are confined at the top of the two loops, where the magnetic field is lower.

The hypothesis of the presence of two loops is supported by optical observations of UX Ari (Vogt & Hatzes 1991; Elias et al. 1995), that indicate the presence of a polar spot and a series of spots located in an equatorial band. The orientation of the two radio components, which are nearly perpendicular to each other, suggests the following scenario: the stronger emission comes from a meridian loop, with one foot anchored on the visible polar spot, while the weaker source corresponds to an equatorial loop. As the star rotates, the two loops change their relative position and orientation with respect to the line of sight, causing the observed variations of the source structure. We note that this loop geometry is perfectly compatible with the one suggested by Trigilio et al. (1998) to interpret their observations of January 1993.

In Fig. 7 we show a sketch of the possible geometry of the two loops at the time of our VLBI observations, inferred from the model components of Table 1. The darker regions at the top of the loops represent the possible location of the two source components (i.e. the two ellipses in the lower left corners of Fig. 6). We remark that this is only a sketch, since it is not possible to determine the exact source geometry from our data. It is possible that the size of the loops does not remain constant during the full period; for example, one or both loops could

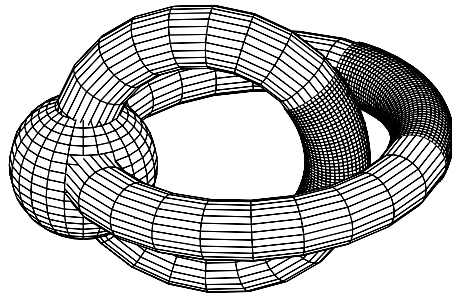
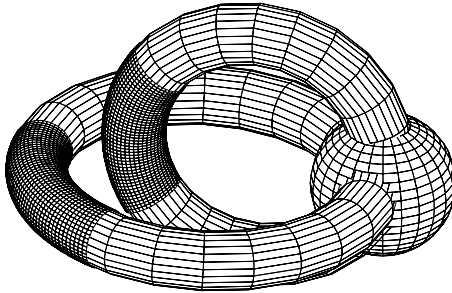
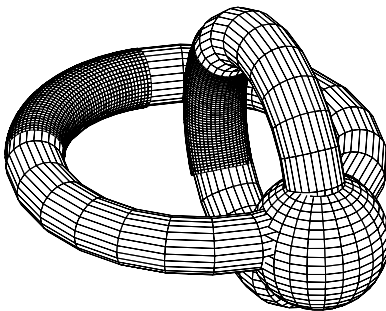
A: $\phi = 0.75$ B: $\phi = 0.21$ C: $\phi = 0.37$

Fig. 7. A sketch of the possible geometry for the two emitting loops at the time of the three VLBI observations. The corresponding orbital phases are $\phi = 0.75$ (A), 0.25 (B) and 0.37 (C). The darker regions at the top of the loops represent the possible location of the two source components (i.e. the two ellipses in the lower left corners of Fig. 6)

expand outwards, contributing to the increase in the angular separation of the source components. Moreover the position of the loop feet could be different from that shown: for instance the meridian loop does not have to go necessarily from pole to pole, but it could go from pole to equator.

As shown in Table 1, the flux density of the two components decreases with time reaching a minimum at $\phi = 0.37$. Could the occultation by the star play a role in this decreasing? As shown in Massi et al. (1998), the only case in which the star really occultates the radio source is around phase 0.4, when the bright compact component associated with the loop feet disappears behind the star. Emission below 100 mJy, which is associated

with the rest of the loop, remains always observable and is not significantly affected by the stellar rotation. Fig. 7c fits quite well this scenario, since the two components at the top of the loops remain completely unobscured at this phase. We conclude that the observed decrease of the flux density with time is due to the flare decay only.

5. Conclusions

In this paper we have reported the results of three 5 GHz VLBI observations of UX Ari, performed in September 1993 during five consecutive days. The star was undergoing a moderate flare with a peak flux density of $\sim 60\text{--}70$ mJy just after the first VLBI run, which decayed to a minimum three days later, at the time of the last observation.

The maps show a clear variation of the source structure with time. A model fitting of both the visibility amplitudes and the maps indicates that the radio source consists of two components of different flux densities but nearly equal sizes. There is no evidence of a compact source, in agreement with other recent results (Trigilio et al. 1993; Beasley & Bastian 1996). The two source components are presumably associated with two different loops anchored on the active K star. Since the observations have been made at different orbital phases (0.75, 0.21 and 0.37) we can interpret the changes in the source structure as due to the varying position of the two loops with respect to the line of sight as the star rotates. Since the source is extended, the modulation of the emission induced by the stellar rotation is negligible, and the observed decrease of the flux density with time can be ascribed to the decay of the flare due to energy losses. However, during strong flares, when a compact component is present, geometrical effects become important: in order to study this effect, we plan to perform new VLBI observations during a strong flare, with a more complete temporal coverage.

Acknowledgements. We thank Tim Bastian for his comments and suggestions as referee of this paper and Franca Chiuderi Drago for helpful discussions and for the careful reading of the manuscript. MM acknowledges support for her research by the European Commission's TMR programme, Access to Large-Scale Facilities, under contract number ERBFMGECT950012. JMP and RE acknowledge partial financial support from DGICYT grant PB94-0904, Spain.

References

- Beasley A.J., Bastian T.S., 1996, In: Pallavicini R., Dupree A.K. (eds.) *Cool Stars, Stellar Systems, and the Sun*. 9th Cambridge Workshop, ASP Conf. Ser. 109, ASP, San Francisco, p. 639
- Carlos R.C., Popper D.M., 1971, *PASP* 83, 504
- Elias N.M. II, Quirrenbach A., Witzel A., et al., 1995, *ApJ* 439, 983
- Franciosini E., Chiuderi Drago F., 1995, *A&A* 297, 535
- Lestrade J.-F., Mutel R.L., Preston R.A., Scheid J.A., Phillips R.B., 1984, *ApJ* 279, 184
- Massi M., Felli M., Pallavicini R., et al., 1988, *A&A* 197, 200
- Massi M., Neidhöfer J., Torricelli Ciamponi G., Chiuderi Drago F., 1998, *A&A* 332, 149
- Mutel R.L., Lestrade J.-F., Preston R.A., Phillips R.B., 1985, *ApJ* 289, 262

- Mutel R.L., Morris D.H., Doiron D.J., Lestrade J.-F., 1987, *AJ* 93, 1220
- Neidhöfer J., Massi M., Chiuderi Drago F., 1993, *A&A* 278, L51
- Torricelli Ciamponi G., Franciosini E., Massi M., Neidhöfer J., 1998, *A&A* 333, 970
- Trigilio C., Umana G., Migenes V., 1993, *MNRAS* 260, 903
- Trigilio C., Leto P., Umana G., 1998, *A&A* 330, 1060
- Vogt S.S., Hatzes A.P., 1991, In: Tuominen I., et al. (eds) *The Sun and Cool Stars: Activity, Magnetism, Dynamos*. IAU Coll 130, Springer, Berlin, p. 297